Title	Band gap engineering of (N, Ta)-codoped TiO2 : a first-principles calculation
Author(s)	Long, Run; English, Niall J.
Publication date	2009-07-29
Publication information	Chemical Physics Letters, 478 (4-6): 175-179
Publisher	Elsevier
Link to online version	http://dx.doi.org/10.1016/j.cplett.2009.07.084
Item record/more information	http://hdl.handle.net/10197/2719
Publisher's statement	All rights reserved.
Publisher's version (DOI)	http://dx.doi.org/10.1016/j.cplett.2009.07.084

Band gap engineering of (N, Ta)-codoped TiO_2: A first-principles calculation

Run Long and Niall J. English[a)]

The SEC Strategic Research Cluster and the Centre for Synthesis and Chemical Biology, Conway Institute of Biomolecular and Biomedical Research, School of Chemical and Bioprocess Engineering, University College Dublin, Belfield, Dublin 4, Ireland

Abstract: The electronic properties and photocatalytic activity of X (N, C) / transition metal (TM=Ta, Hf, Fe) – codoped anatase TiO_2 have been investigated using density functional theory. It was found that only the (N, Ta)-codoping case narrows the band gap significantly by about 0.**48** eV, driven by the **continuum-like p-d hybridized** states **above** the top of valence band and d states at the bottom of conduction band. The calculated energy results suggest that codoping of Ta with N can increase the N concentration in N-doped TiO_2 based on energy results.

Keywords: (N, Ta)-doped, electronic structure, TiO_2

[a)] Corresponding author. Electronic Mail: niall.english@ucd.ie

Titania (TiO_2)-based photocatalysts have received intense attention as promising photocatalytic materials for decomposition of organic pollutants present in water or air [1]. However, as a wide band gap semiconductor (3.20 eV), anatase allows only absorption of ultraviolet irradiation, which amounts to ~5% of solar energy. Further, its photoexcited electron-hole pairs recombine relatively easily. Both of these factors limit somewhat its possible applications in photocatalysts. Therefore, the extension of optical absorption in TiO_2-based materials to the visible-light region, in conjunction with a low photogenerated electron-hole recombination rate, is of great practical importance.

A popular field of investigation is the use of suitable dopants to address this problem to a certain degree. Nitrogen-doped TiO_2 is considered to be one of the most effective photocatalysts and it has been investigated widely, both by experimental and theoretical methods [2]. However, due to strongly localized N 2p states at the top of valence band [3], the photocatalytic efficiency of N-doped TiO_2 decreases because isolated empty states tend to trap photogenerated electrons, thereby reducing the photogenerated current [4]. On the other hand, transition metal doping can promote photocatalytic efficiency, but it also suffers from the existence of a carrier recombination center and the formation of strongly localized d states in the band gap, which reduces the carrier mobility significantly [5, 6]. Recently, Gai et al. [7] proposed using passivated codoping of nonmetal and metal elements to extend the TiO_2 absorption edge to the visible light range; because the defect bands are passivated, they will not be active as carrier recombination centers [8]. Our recent

work on (N,W)-doped anatase TiO_2 has also suggested that a continuum band is formed at the top of the valence band, and that W 5d orbitals locate below Ti 3d orbitals in the bottom of conduction band, which narrows the band gap significantly and enhances visible light absorption [9]. **Indeed, before these studies, some other work on (N, F)-codoped TiO_2, (Cr, Sb)-codoped TiO_2, and (N, H)-codoped TiO_2 were reported by different research groups [10-12]. In particular, Di Valentin et al. [10, 11] have shown hybrid density functional technique can properly describe the electronic structures of (N, F)- and (Cr, Sb)-codoped TiO_2, and pointed out (N, F)-codoping reduced the energy cost of doping and the amount of oxygen vacancies in the lattice, as a consequence of the charge compensation between the acceptor N and donor F dopants. In the (Cr, Sb) codoping case, electron transfer from the Sb-related states to the Cr 3d levels is responsible for the enhanced photostability of the (Cr, Sb)-codoped system. However, there are still some impurity states located in the band gap, which reduce the photocatalytic activity somewhat. Mi et al. [12] reported that (N, H) codoping yields significant band gap narrowing and cancels the gap states using generalized gradient approximation (GGA) and confirmed by the experiment. These findings are very similar with our previous result of (N, W)-codoped TiO_2 [9].**

In principle, although there are a few reports on Ta- and (N, Ta)-doped TiO_2 for applications in photocatalytic materials [**13**, **14**], they show that both the photocatalytic activities of Ta-doped TiO_2 [**13**] are enhanced substantially vis-à-vis Degussa P-25 and (N, Ta)-doped TiO_2 has higher oxidation power than that of that of

N-doped TiO_2 under visible light irradiation [**14**]. On the other hand, metal oxynitrides with valence bands composed of hybridized N 2p and O 2p orbitals are one promising class of candidates for visible-light-responsive photocatalysts. For example, TaON was reported to absorb light of wavelength up to 530 nm [**15**]. N-doped Ta_2O_5 can decompose organic compounds under visible light irradiation, as N-doped TiO_2 [**16**]. $BaTaO_2N$ has a perovskite structure, in which the top of the valence band (VBM) consists of hybridized N 2p and O 2p states, whereas the bottom of conduction band (CBM) is composed mainly of empty Ta 5d states [**17**]. It may be speculated that the addition of Ta into N-doped TiO_2 should passivate isolated **N 2p** impurities **empty** states and Ta 5d states localized at the edge of the CBM. In addition, because N^{3-} and Ta^{5+} were substituted at O^{2-} and Ti^{4+} sites, respectively, charge compensation can be expected by (N, Ta) codoping, which should lead to improvement of photocatalytic efficiency. If so, this would serve to reduce substantially the band gap of (N, Ta)-doped TiO_2.

In the present work, the electronic properties of (X, TM) (X = N, C; TM= Ta, Hf, Fe)-codoped TiO_2 have been investigated using density functional theory (DFT) calculations in order to reveal the microscopic mechanisms of band gap narrowing. The electronic structures show that only the (N, Ta)-codoped system displays obvious synergistic effects **with the formation of continuum-like fully occupied** states. Therefore, we shall restrict our discussion primarily to the (N, Ta)-codoped case, and also discuss its thermodynamic properties for both single-element and co-doping from an analysis of the calculated formation energies.

All of the spin-polarized DFT calculations were performed using projector augmented wave (PAW) pseudopotentials as implemented in the Vienna ab initio Simulation Package (VASP) code [**18**, **19**]. The Perdew and Wang parameterization [**20**] of the generalized gradient approximation (GGA [**21**] was adopted for the exchange-correlation potential. The electron wave function was expanded in plane waves up to a cutoff energy of 400 eV and a Monkhorst–Pack *k*-point mesh [**22**] of 4 × 4 × 4 was used for geometry optimization [**23**, **24**] and electronic property calculations. **Both atomic positions and cell parameters were optimized with GGA and GGA + U methods [25] until the residual forces were below 0.01 eV/Å. As will be shown in section 3, the GGA calculations on the geometry parameters agree better with experiments than the GGA + U method. The DFT + U approach introduces an intra-atomic electron-electron interaction as an on-site correction in order to describe systems with localized d and f electrons, which can produce better band gaps relative to GGA. Here the effective on-site Coulomb interaction U = 6.3 eV for Ti 3d and U = 5.0 eV for TM d electron in the GGA + U approach [7].** The calculated band gap of pure anatase is 3.14 eV, which agrees well with the experimental value of 3.20 eV.

The doped systems were constructed from a relaxed **(3 × 3 × 1) 108**-atom anatase supercell. The O atom was replaced by N and the Ti by Ta. (N, Ta)-codoped TiO_2 was modeled by single substitution of N for one O atom, and its adjacent Ti atom was replaced by one substitution of a Ta atom per supercell; calculations showed that the formation of an adjacent N-Ta pair is energetically favorable with respect to other

N-Ta configurations. Other (co)doped systems were created and analyzed in the same way. The supercell model is shown in Fig. 1.

We investigate firstly the structure parameters of anatase TiO_2 using GGA and GGA + U methods. The optimized unit cell parameters are summarized in Table 1, and were *a* = 3.800 Å and *c* = 9.481 Å for pure anatase with the GGA method and *a* = 3.893 Å and *c* = 9.529 Å with GGA+U technique. Although both methods overestimate the lattice parameters with respect to the experimental value *a* = 3.782 Å and *c* = 9.502 Å [26], the GGA results are better than those of the GGA+U method. In the local TiO_6 octahedron, the four equivalent Ti-O bond lengths are 1.938 vs 1.982 Å and the two apical Ti-O bond lengths are 1.998 vs 2.012 Å for the GGA and GGA +U calculations, respectively. The GGA calculated values also agree well with experiment [26]. Therefore, the electronic properties of doped systems in the present work, we first optimized their lattice parameters and atomic positions using the GGA method and then performed GGA + U calculations on electronic properties using the GGA optimal geometry. This method can get a good description of the electronic properties of C-codoped TiO_2 by Dai et al. [27].

To examine the relative difficulty for different ions to incorporate into the lattice, we calculated the dopant formation energies. The formation energy was calculated according to the formula (1)

$$E_{form} = E(doped) - E(pure) - \mu_N - \mu_{Ta} + \mu_O + \mu_{Ti} \quad (1)$$

where $E(doped)$ and $E(pure)$ are the total energies with and without dopants. The

chemical potentials for O (μ_O), Ti (μ_{Ti}), and N(μ_N) atoms were taken from our previous study [9]. The chemical potential for μ_{Ti} was calculated based on the formula $\mu_{TiO_2} = \mu_{Ti} + \mu_{O_2}$ .The chemical potential for the Ta atom μ_{Ta} was estimated from that of bulk metal tungsten ($\mu_{Ta} = \mu_{Ta}^{metal}$). The calculated formation energies under Ti- and O-rich growth conditions are summarized in Table I. Their order suggests that: 1) N occupies the O site preferentially under Ti-rich conditions; 2) Ta is substituted easily under both Ti- and O-rich conditions; 3) the incorporation of Ta promotes N doping under both Ti- and O-rich conditions. It should also be noted that the formation energies of (N, Ta)-codoped TiO_2 are both negative. Therefore, to enhance N concentration in N-doped TiO_2, one may select Ta as its codopant in experiments. The electronegativity and ionic radius of Ta^{5+} (1.50, 0.064 nm) and Ti^{4+}(1.54, 0.061 nm) are similar: the Ta ion concentration in Ta-doped TiO_2 can reach a higher level, which has been confirmed by recent experimental work that achieved ultrahigh Ta concentration in $Ti_{1-x}Ta_xO_{2+x/2}$ (x=0.025, 0.05, and 0.075) [**13**].

To modify the band edge structure of TiO_2 through doping, we first need to know their compositions. Hence, we calculated the density of states (DOS) and the projected density of states (PDOS) (cf. Figs. 2a & 2e). It shows that the valence band edge of TiO_2 consists mainly of O 2p states while the conduction band edge is dominated by Ti 3d states. Hence, incorporation of the N and Ta atoms should modify the CBM and VBM, respectively, due to their having different p and d orbitals with respect to O 2p and Ti 3d states.

For N-doped TiO_2 (cf. Figs. 2b & 2f), substitution of N at the O site acts as a single

acceptor due to N having one less electron than O, leading to acceptor N 2p states located above the VBM of TiO_2. However, the VBM and CBM of N-TiO_2 exhibit no change with respect to the undoped case. In this case, the gap state is responsible for photocatalytic activation under visible-light irradiation. However, this gap state can act as a recombination center to limit the efficiency of N-doped TiO_2 in the visible light region. For Ta-doped TiO_2 (cf. Figs. 2c & 2g), shallow donor levels are created near the CBM and the impurity Ta 5d states lie below the host Ti 3d states. This led to a small reduction in the band gap by about 0.1 eV. The shallowness of the 5d orbital energy vis-à-vis the 3d orbital is related to the more delocalized character of the 5d orbital. Therefore, when Ti is replaced by Ta, the defect levels coincide with the conduction band; Ta is a suitable n-type dopant that modifies the CBM little. In addition, shallow donor states would be expected to extend slightly the absorption edge to the visible light range; this serves to explain recent experimental work in which Ta-doped TiO_2 was noted to exhibit better photocatalytic activity with respect to Degussa P-25 [**13**]. As mentioned previously, Fig. 2a shows that the valence band edge consists mainly of O 2p states, whereas the conduction band edge is composed predominately of Ti 3d states. Therefore, codoping with N and Ta would be expected to modify the conduction and valence band edges simultaneously because N has a different atomic p orbital energy relative to O, and Ta has a different atomic d orbital energy vis-à-vis Ti.

For (N, Ta)-codoped TiO_2 (cf. Figs. 2d and 2f), it is significant that a hybridized N2p-Ta5d state is formed **below the Fermi level E_F**, which **means that fully**

occupied hybridized states appear in contrast to single doping **(empty states)**; these **fully occupied states** in the valence band edge **cannot act as recombination centres. This effect is very similar to the continuum bands observed in (N, H)- and (N, W)-doped TiO2 and thus may be labeled as continuum-like band [9, 12]**. Conversely, partial Ta 5d states are located at the edge of the conduction band. This reduces the band gap substantially by about **0.48** eV. The **continuum-like** nature of the band suggests that carrier recombination rates with holes may be reduced, which would serve to promote visible light absorption. Incorporation of Ta into N-doped TiO_2 changes the character of N 2p orbitals from isolated empty midgap states to **fully occupied** N 2p-**Ta 5d hybridized** states **above** the top of the valence band, while the Ta 5d state is located at the conduction band edge. This rationalizes recent experimental data which showed that (N, Ta)-doped TiO_2 exhibits higher visible-light photocatalytic efficiency than N-doped TiO_2 [**14**]. To study further the components of the **fully occupied hybridized states** and CBM, **the band structure and its corresponding** partial charge **of the gamma point** of (N, Ta)-doped TiO_2 obtained by **GGA + U** calculations **are** shown in Fig. 3. **The band structure (cf. Fig 3a) shows that isolated impurity states lie above the host VBM and below the Fermi level E_F, i.e. for the highest occupied molecular orbital, the electron transfer from the fully occupied states to the CBM will reduce the photon transition energy significantly (cf. Fig. 3a).** As expected, the hybridized states (cf. **Fig. 3b**) **arise from** N 2p, Ta 5d, **and a few O 2p** orbitals, whereas the CBM (cf. Fig. **3c**) is composed primarily of empty Ta 5d and Ti 3d orbitals. The N-Ta-O linkage leads to the

formation of a continuum-like band which can enhance further visible light absorption in (N, Ta)-codoped TiO_2. To probe the origin of band gap modifications of (N, Ta)-codoped anatase, we have plotted the total charge and spin density on the (100) surface in Fig. 4. The electron density is localized mostly on the N, indicating that there should be some electron transfer from Ti and Ta atoms to N atoms (cf. Fig. 4a), while the spin density is very small and significantly dispersed (cf. Fig. 4b) **because formation of an N-Ta bond cancels the unpaired electrons of N.** This induces that the spin density of an N atom couples with that of the adjacent Ta, resulting in hybridization of the N 2p with Ta 5d states (cf. Figs. 2d & 4b). These characteristics are very different from single N-doped TiO_2 [9]. **The total energies of (N, Ta)-codoped TiO_2 are the same with spin-polarized and nonspin-polarized calculations, which also indicates that the addition of Ta into N-doped TiO_2 cancels the spin polarization.** Bader charges [**28**, **29**] are summarized in Table II. They show that the N ion has a charge of -1.37 |e| for N-doping, while it is **-2.11** |e| for (N, Ta)-codoping, with more electrons transferring from the Ta and adjacent Ti atoms to the N ion. The bond length of N-Ta is **1.977** Å, which is shorter than that of the N-Ti length of **2.063** Å for N-doping. This indicates further that a strong N-Ta bond forms in (N, Ta)-codoped TiO_2. The calculated results suggest that (N, Ta)-codoped TiO_2 is a very promising photocatalytic material. To examine the stability of (N, Ta) defect pair, we calculated the defect pair binding energy [**30**]

$$E_b = E(Ta@Ti) + E(N@O) - E(Ta@Ti + N@O) - E(TiO_2) \qquad (2)$$

Positive E_b indicates that the defect pair tends to bind to each other and is stable.

The calculated binding energy for the (N, Ta) pair is **1.50** eV, indicating that this impurity pair is stable vis-à-vis isolated dopants. The large binding energy results from charge transfer from Ta to N and the strong associated Coulomb interaction between positively-charged Ta and negatively-charged N. The above Bader charges confirmed the findings from the binding energy.

As mentioned earlier, we also investigated other codoped systems besides (N, Ta)-codoped TiO_2, such as (C, Ta), (C, Hf), (C, Fe), (N, Hf), and (N, Fe)-codoped cases. However, their DOS [cf. Figure 5] show that all of the systems do not possess the favorable characteristics similar to (N, Ta) despite their band gaps narrowing to varying degrees; gap states are introduced into the band gap, which could serve to act as effective recombination centers. This suggests that the photocatalytic activity of these codoped systems would be inferior to that of (N, Ta)-codoped TiO_2.

In conclusion, we have carried out a first-principles study to evaluate the energetic and electronic properties of N-, Ta-, and (N, Ta)-doped anatase TiO_2. Incorporation of Ta into N-doped TiO_2 leads to **formation of continuum-like fully occupied N2p-Ta 5d hybridized states above** the top of valence band as well as Ta 5d orbitals located at the bottom of the conduction band, and reduces the band gap significantly. The band gap narrowing would serve to contribute to the enhancement of optical absorption under visible light irradiation. The calculated energetic results indicate that codoping of N with Ta can effectively reduce the formation energy and enhance N concentration. The results suggest that (N, Ta)-codoped TiO_2 is a very promising photocatalytic material.

This work was supported by the Irish Research Council for Science, Engineering and Technology (IRCSET).

References

[1] M. R. Hoffmann, S. T. Martin, WW. Choi, D. W. Bahnemann, Chem. Rev. 95(1995) 69.

[2] R. Asahi, T. Morikawa, T. Ohwaki, K. Aoki, Y. Taga, Science 293 (2001) 269.

[3] H. Irie, Y. Watanabe, K. Hashimoto, J. Phys. Chem. B 107 (2003) 5483.

[4] Z. Lin, A. Orlov, R. M. Lambert, and M. C. Payne, J. Phys. Chem. B 107(2003) 5483.

[5] J. M. Herrmann, J. Disdier, and P. Pichat, Chem. Phys. Lett. 108 (1984) 618.

[6] W. Mu, J. M. Herrmann, and P. Pichat, Catal. Lett. 3 (1989) 73.

[7] Y. Q. Gai, J. B. Li, A. S. Li, J. B. Xia, S. H. Wei, Phys. Rev. Lett. 102 (2009) 036402.

[8] K. S. Ahn, Y. Yan, S. Shet, T. Deutsch, J. Turner, and M. Al-Jassim, Appl. Phys. Lett. 91 (2007) 231909.

[9] R. Long, N. J. English, Appl. Phys. Lett. 94 (2009) 132102.

[10] C. Di Valentin, E. Finazzi, and G. Pacchioni, Chem. Mater. 20 (2008) 3706.

[11] C. Di Valentin, G. Pacchioni, H. Pnishi, and A. Kudo, Chem. Phys. Lett. 469 (2009) 166.

[12] L. Mi, P. Xu, H. Shen, and P. N. Wang, Appl. Phys. Lett. 90 (2007) 171909.

[13] C. H. Wang, A. F. Geng, Y. H. Guo, S. J. Jiang, X. S. Qu, Mater. Lett. 60 (2006)

[14] K. Obata, H. Irie, K. Hashimoto, Chem. Phys. 339 (2007) 124.

[15] R. Nakamura, T. Tanaka, Y. Nakato, J. Phys. Chem. B 109 (2005) 8920.

[16] M. Takashi, I. Hiroshi, H. Kazuhito, J. Phys. Chem. B 108 (2004) 15803.

[17] M. Kazuhiko, D. Kazunari, J. Phys. Chem. C 111 (2007) 7851.

[18] G. Kresse, J. Hafner, Phys. Rev. B 47 (1994) 558.

[19] G. Kresse, J. Furtherműller, Phys. Rev. B 54 (1996)11169.

[20] J. P. Perdew, K. Burk, M. Ernzerhof, Phys. Rev. Lett. 77 (1996) 3865.

[21] J. P. Perdew, Y. Wang, Phys. Rev. B 45 (1992) 13244.

[22] H. J. Monkhorst, J. D. Pack, Phys. Rev. B 13 (1976) 5188.

[23] E. R. Davidson, *Methods in Computational Molecular Physics* edited by G.H.F. Diercksen, Reidel, Dordrecht, 1983

[24] S. Wilson, Vol. 113 *NATO Advanced Study Institute, Series C* (Plenum, New York, 1983), p. 95.

[25] S. L. Dudarev, G. A. Botton, S. Y. Savarsov, C. J. Humphreys, and A. P. Sutton, Phys. Rev. B 57 (1998) 1505.

[26] J. K. Burdett, T. Hughbandks, G. J. Miller, J. W. Richardson, J. V. Smith, J. Am. Chem. Soc. 109 (1987) 3639.

[27] K. S. Yang, Y. Dai, B. B. Huang, and M. –H. Whangbo, J. Phys. Chem. C 113 (2009) 2624.

[28] G. Henkelman, A. Arnaldsson, H. Jónsson, Comput. Mater. Sci. 36 (2006) 354.

[29] E. Sanville, S. D. Kenny, R. Smith, and G. Henkelman, J. Comp. Chem. 28 (2007)

[30] J. Li, S. H. Wei, S. S. Li, and J. B. Xia, Phys. Rev. B 74 (2006) 081201.

Table I Formation energies (eV) E_{form} for N-, Ta-, and (N, Ta)-doped TiO_2.

		Ti-rich	O-rich
E_{form}	*N-doped*	***0.63***	***5.64***
E_{form}	*Ta-doped*	***0.02***	***-9.98***
E_{form}	*(N, Ta)-doped*	***-0.85***	***-5.85***

Table II Average Bader Charges **(**|e|**)** on dopant atoms and their adjacent atoms in N- and (N, Ta)-doped TiO_2. The number in parenthesis denotes the number of atoms around the dopant.

	N-doped	(N, Ta)-doped
N	*-1.37*	*-2.**11***
Ta		***4.66***
O		***-1.61**(5)*
Ti	***2.74**(3)*	***2.75** (2)*

Figure Captions

Figure 1. Supercell model for defective anatase TiO_2 showing the location of the dopants. The ion doping sites are marked with N and Ta. The large light spheres and the small red spheres represent the Ti and O atoms, respectively.

Figure 2. DOS(left) for (a) pure TiO_2, (b) N-doped TiO_2, (c) Ta-doped TiO_2, and (d) (N, Ta)-doped TiO_2. The corresponding PDOS (right) are shown on the right in (e)-(h). The PDOS plots of (e)-(h) are enlarged for clarity. The top of valence band of pure TiO_2 is taken as the reference level. **The dashed line represents the Fermi level E_F.**

Figure 3 (a) Band structure and partial electron densities of (b) highest occupied molecular orbital and (c) CBM at gamma point of (N, Ta)-doped TiO_2. The dashed line in (a) is the Fermi level E_F.

Figure 4 (a) Electron densities and (b) spin densities on the (100) surface for (N, Ta)-doped TiO_2.

Figure 5 DOS for (a) (C, Ta), (b) (C, Hf), (c) (C, Fe), (d) (N, Hf), and (e) (N, Fe)-codoped TiO_2. The top of valence band of pure TiO_2 is taken as the reference level (not shown).

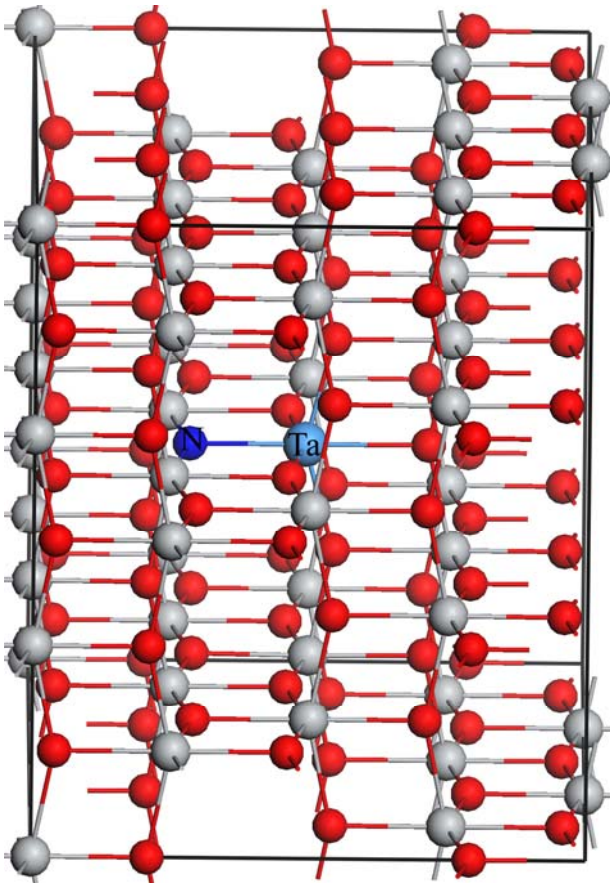

Figure 1

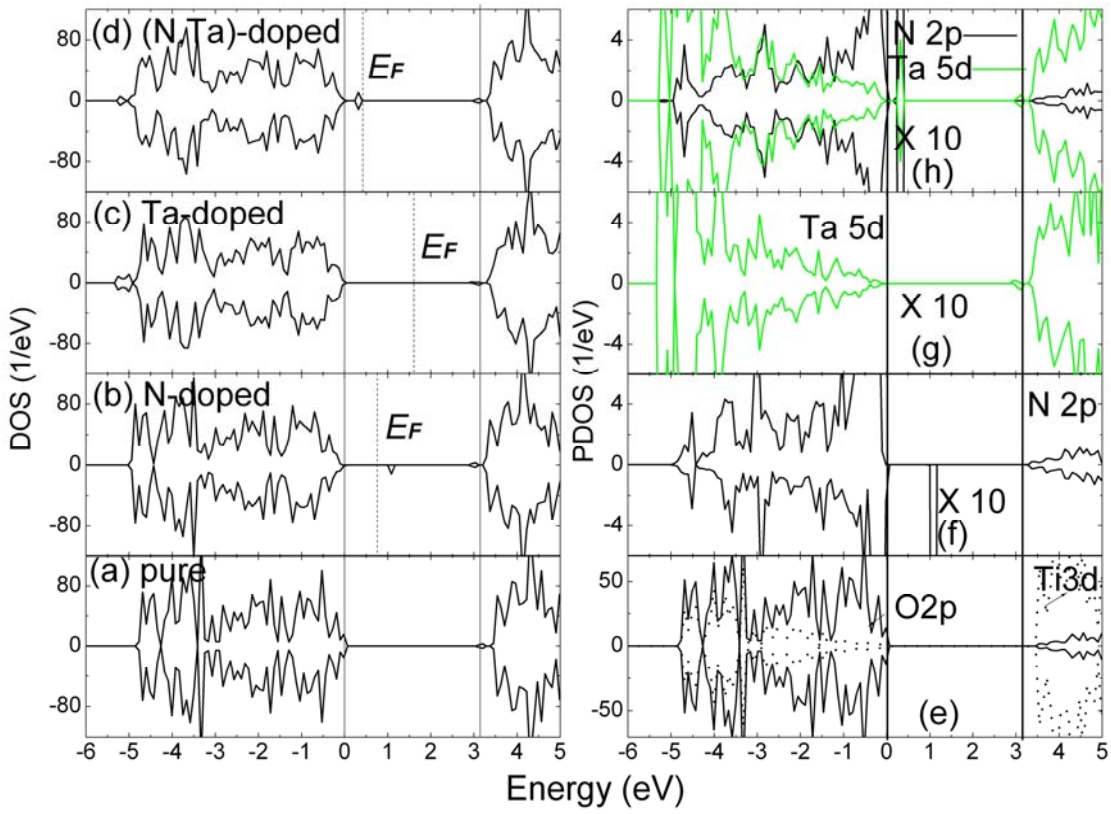
(d) (N,Ta)-doped
(c) Ta-doped
(b) N-doped
(a) pure
EF
DOS (1/eV)
PDOS (1/eV)
N 2p
Ta 5d
X 10
(h)
Ta 5d
X 10
(g)
N 2p
X 10
(f)
O2p
Ti3d
(e)
Energy (eV)

Figure 2

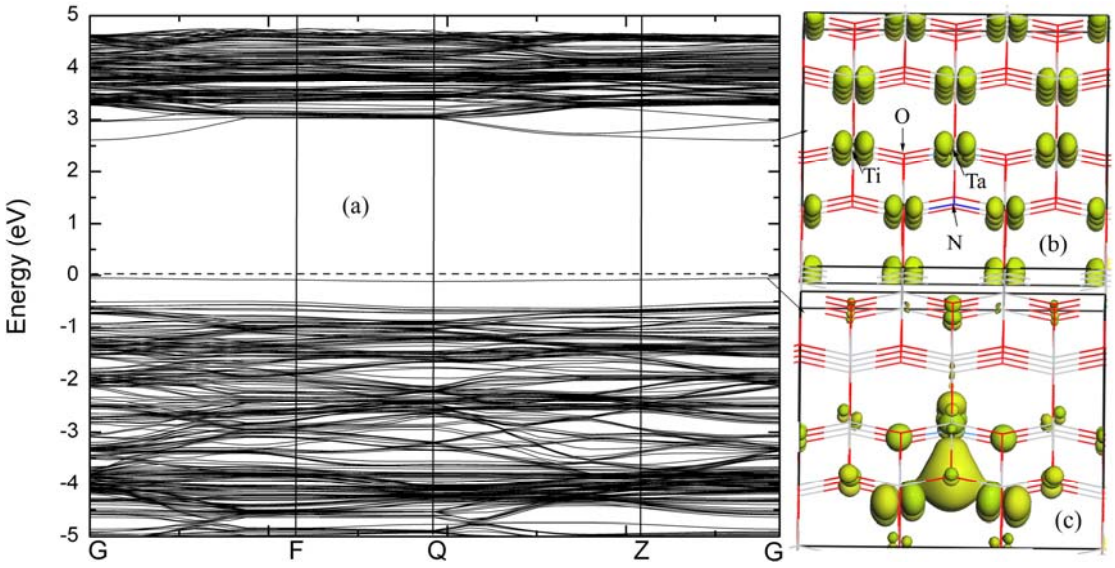

Figure 3

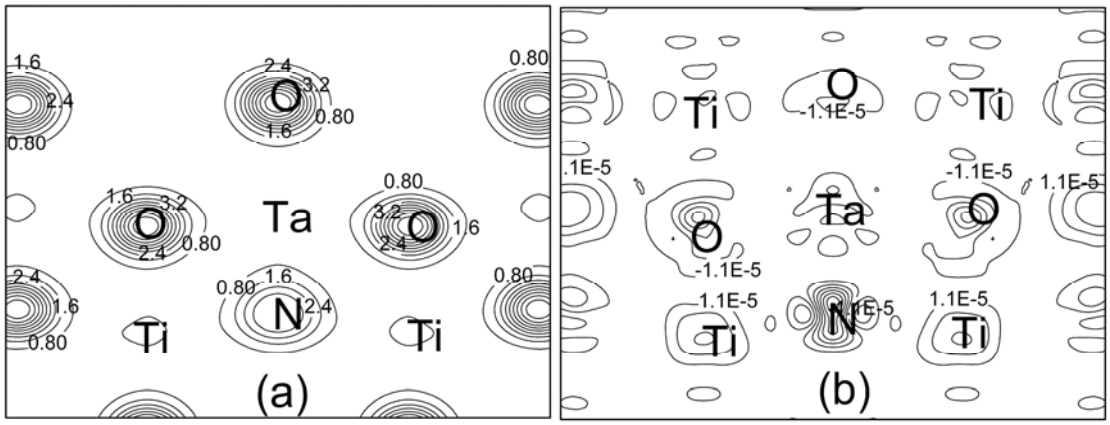
1.6
2.4
0.80
2.4
3.2
O
1.6
0.80
0.80
1.6
3.2
O
2.4
0.80
Ta
0.80
3.2
O
2.4
1.6
2.4
1.6
0.80
0.80
1.6
N
2.4
0.80
Ti
Ti
(a)
Ti
O
-1.1E-5
Ti
.1E-5
-1.1E-5
1.1E-5
Ta
O
O
-1.1E-5
-1.1E-5
1.1E-5
1.1E-5
Ti
N
Ti
(b)

Figure 4

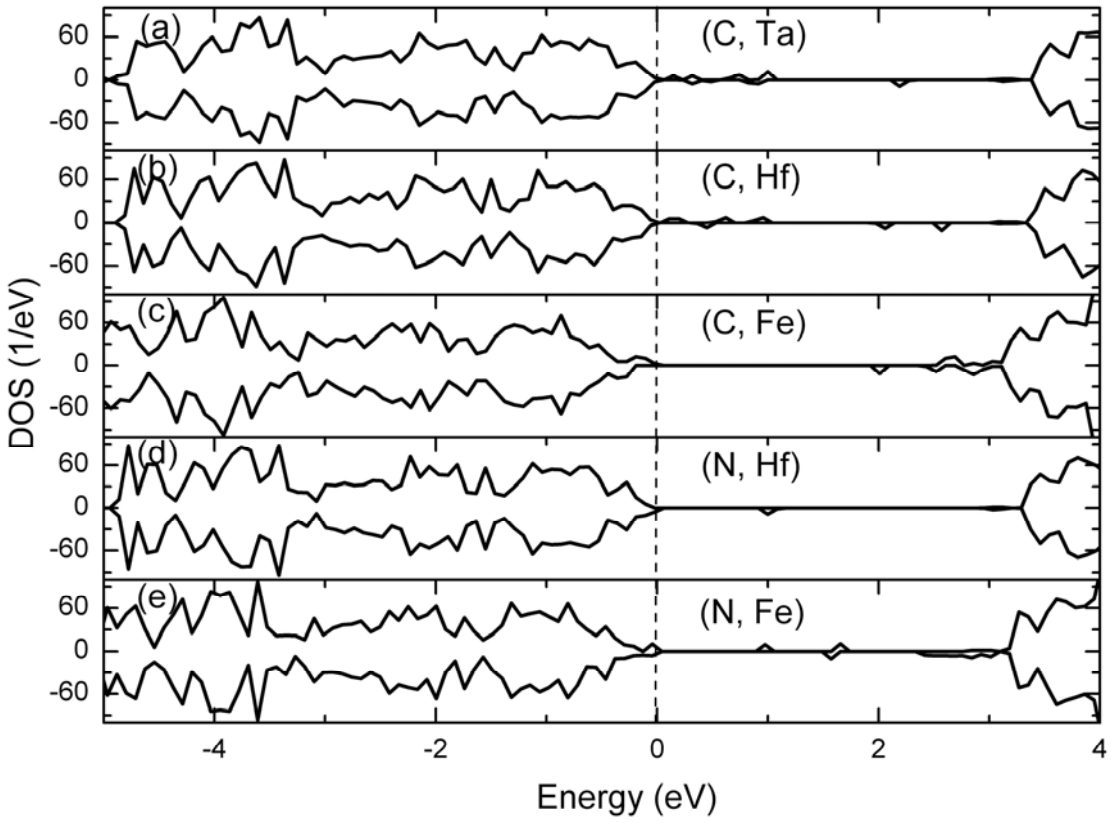

Figure 5